

# Cropland expansion drives vegetation greenness decline in Southeast Asia

Ruiying Zhao<sup>1\*</sup>, Xiangzhong Luo<sup>1,2\*</sup>, Yuheng Yang<sup>1</sup>, Luri Nurlaila Syahid<sup>1</sup>, Chi Chen<sup>3</sup>, Janice Ser Huay Lee<sup>4</sup>

5 <sup>1</sup>Department of Geography, National University of Singapore, 117570, Singapore

<sup>2</sup>Center for Nature-based Climate Solutions, Department of Biological Sciences, National University of Singapore, 117558, Singapore

<sup>3</sup>Department of Ecology, Evolution, and Natural Resources, School of Environmental and Biological Sciences, Rutgers University, New Brunswick, NJ 08901, USA

10 <sup>4</sup>Asian School of the Environment and Earth Observatory of Singapore, Nanyang Technological University, 637459, Singapore

*Correspondence to:* Ruiying Zhao ([ruiying@nus.edu.sg](mailto:ruiying@nus.edu.sg)); Xiangzhong Luo ([xzluo.remi@nus.edu.sg](mailto:xzluo.remi@nus.edu.sg))

**Abstract.** Land use and land cover change (LUCC) is a key factor in determining regional vegetation greenness, impacting terrestrial carbon, water, and energy budgets. As a global hotspot of LUCC, Southeast Asia has experienced intensive cropland and plantation expansions in the past half-century, yet their impacts on regional greenness have not been elucidated. Here, we harmonized multiple land cover datasets, and used satellite-derived leaf area index (LAI) in combination with a machine learning approach to quantify the impacts of LUCC on vegetation greenness in insular Southeast Asia (i.e., Peninsular Malaysia, Sumatra, and Borneo islands). We found that regional LAI shows almost no trend ( $0.04 \times 10^{-2} \text{ m}^2 \text{ m}^{-2} \text{ yr}^{-1}$ ) from 2000 to 2016, as a net effect of increased LAI ( $+5.71 \times 10^{-2} \text{ m}^2 \text{ m}^{-2} \text{ yr}^{-1}$ ) due to CO<sub>2</sub> fertilization, offset by decreased LAI mainly due to cropland expansion ( $-4.46 \times 10^{-2} \text{ m}^2 \text{ m}^{-2} \text{ yr}^{-1}$ ). The impact of croplands on greenness in Southeast Asia contrasts with that in India and China. Meanwhile, oil palm expansion and climate change induced only small decreases in LAI in Southeast Asia ( $-0.41 \times 10^{-2} \text{ m}^2 \text{ m}^{-2} \text{ yr}^{-1}$  and  $-0.38 \times 10^{-2} \text{ m}^2 \text{ m}^{-2} \text{ yr}^{-1}$ , respectively). Our research unveils how LAI changes with different processes of LUCC in Southeast Asia and offers a quantitative framework to assess vegetation greenness under different land use scenarios.

## 25 **1 Introduction**

Terrestrial vegetation plays a pivotal role in regulating ecosystem services, conserving biodiversity, and mitigating climate change impacts. Over recent decades, long-term satellite records of the leaf area index (LAI) have disclosed a notable increase in vegetation greenness on Earth (Chen et al., 2019; Zhu et al., 2016). While at the global scale, elevated atmospheric CO<sub>2</sub> concentrations and climate change are regarded as the driving factors for vegetation greening (Zhu et al., 2016), at the regional scale, land use and land cover change (LUCC) can also substantially impact greenness. Previous studies have found that cropland intensification and afforestation are the primary drivers for the greening in India and China (Chen et al., 2019;

Kuttiipurath and Kashyap, 2023). Meanwhile, other studies reported that deforestation for croplands or pastures serves as a key driver for decreasing greenness in the Amazon (Chen et al., 2019; Querino et al., 2016). Thus, the LUCC can either increase or decrease vegetation greenness, depending on the prior land use (e.g., forests, pastures), the subsequent land use (e.g., croplands, pastures, and plantations), and the intensity of these land uses (Wang and Friedl, 2019).

Southeast Asia harbours diverse biodiversity and ecosystems. Yet, the trends and drivers of regional greenness remain largely underexplored. Previous studies reveal that CO<sub>2</sub> fertilization is a primary driver of the greening trend in Southeast Asia within a global context (Chen et al., 2022; Chen and Guestrin, 2016). Climate change, especially temperature rise, could reduce vegetation growth in the tropics (Piao et al., 2020) or drive green-up in maritime Southeast Asia during El Niño (Satriawan et al., 2024). More importantly, land-use change, particularly deforestation, is the predominant factor causing the decline of greenness in tropical countries like Indonesia (Chen et al., 2019; Piao et al., 2020). However, these studies primarily focused on a global scale and likely oversimplified regional dynamics, such as complex land use processes.

Since the 1950s, Southeast Asia has been a global hotspot of LUCC (Houghton and Nassikas, 2017), with maritime countries such as Indonesia and Malaysia having the greatest deforestation rates in the world (Harris et al., 2012). An increase in food crops and export-oriented crop production has driven a significant transformation of tropical forests into commodity plantations like oil palms or croplands for food (Fagan et al., 2022; Zeng et al., 2018). Indonesia and Malaysia are the largest producers of palm fruit, with 250 and 97 million tons of palm fruit produced in 2020 (FAOSTAT, 2022), respectively. Meanwhile, Indonesia and Malaysia experienced tree cover losses of approximately 29.4 and 8.92 million hectares, respectively in the past two decades, equivalent to 18% and 30% of their tree cover in 2000 (Global Forest Watch, <https://www.globalforestwatch.org/>).

Despite the substantial LUCC in the past years, we lack a clear understanding of the impacts of LUCC on vegetation greenness in Southeast Asia. This is partly due to the complexity of the recent land use history of the region. For example, in Indonesia, the dominant LUCC types in the 2000s were the conversion of forests to oil palm plantations and cropland in lowland regions, while in the 2010s, the conversion of forests to oil palm slowed down, shifting more towards highland croplands and the rotation of plantations (Descals et al., 2021; Xu et al., 2020; Zeng et al., 2018). These LUCC processes can differentially affect vegetation greenness and biogeochemical cycles (Ito and Hajima, 2020), with further feedback on vegetation greenness (Wang and Friedl, 2019). However, current studies on the assessment of LUCC impacts do not often distinguish these individual land use processes, but instead categorize the loss of forests under one “deforestation” category (Sitch et al., 2015) or regard plantation as similar to natural forests (Hansen et al., 2013).

In this study, we aim to assess the impact of LUCC on vegetation greenness in Southeast Asia and quantify the contributions of the different LUCC processes to the changes in greenness. We collected and harmonized various types of land cover datasets (Chini et al., 2021; Hansen et al., 2013; Sulla-Menashe et al., 2019; Xu et al., 2020) to build a detailed land use history for Southeast Asia from 2000 to 2016. We further used a machine learning approach to quantify the impacts of land uses on LAI, along with the impacts from climate, CO<sub>2</sub> concentrations, stand age, etc. Our machine learning approach, combined with

65 hypothetical scenarios that simulate vegetation greenness without LUCC processes, enables us to isolate the impacts of  
different land use changes on LAI by estimating the difference between scenario-based LAI.

## 2. Materials and Methods

### 2.1 Study areas

Depending on the availability of various land use data, we focused our study on a region including Peninsular Malaysia,  
70 Sumatra, and Borneo islands (Fig. 1), which experience rapid LUCC in Southeast Asia (Geist and F, 2001; Mao et al., 2023).  
Since the 1980s, insular Southeast Asia has lost at least 1.0% of its forests annually (Felbab-Brown, 2013; Miettinen et al.,  
2011), primarily due to cropland and plantation expansions (Wang et al., 2023; Wicke et al., 2011; Xu et al., 2020). Particularly  
notable is the expansion of oil palm plantations in Indonesia and Malaysia (Chen et al., 2024; Euler et al., 2016). From the  
1990s to the 2010s, the extent of oil palm plantations increased from 1.3 million hectares (Mha) to 7.7 Mha in Indonesia and  
75 from 2.1 to 5.2 Mha in Malaysia (Xu et al., 2022). A national-wide study reported that around 55% to 59% of oil palm  
plantation expansions in Malaysia and at least 56% in Indonesia occurred on lands previously covered by forests during the  
period of 1990 to 2005 (Vijay et al., 2016; Koh and Wilcove, 2008). In parallel, cropland expansion also drives deforestation  
in our study area, with approximately 15% of forest loss in Indonesia attributed to this cause (Austin et al., 2019). Rubber,  
timber, and other plantations have also resulted in deforestation. A recent study revealed that between 2001 and 2016,  
80 approximately 20% of rubber plantations in Indonesia and 33% in Malaysia were established on land previously covered by  
forests, resulting in a loss of about 1 Mha and 0.32 Mha of forest in these countries, respectively (Wang et al., 2023).

### 2.2 Identification of greening trend

Leaf area index indicates the total amount of one-sided leaf area per unit of ground surface area (Chen and Black, 1992;  
Watson, 1947) and often serves as a measure of vegetation greenness (Zhu et al., 2016). In this study, we use the GLOBMAP  
85 LAI dataset, which provides a global record of vegetation cover with a 500 m resolution and is one of the main LAI datasets  
used for global greenness studies (Piao et al., 2020b; Zhu et al., 2016). We used the GLOBMAP LAI (version 3) dataset post  
2001, which was generated based on the Moderate Resolution Imaging Spectroradiometer (MODIS) surface reflectance (Liu  
et al., 2012), with an advanced algorithm to consider canopy clumping, making it particularly suitable for dense canopies in  
the tropics (Fang et al., 2019). To assess the trend of LAI for individual pixels, we utilized the Mann-Kendall Test, a non-  
90 parametric statistical method that can effectively identify consistent upward or downward trends over time (Mann, 1945). This  
test provides the pixel-by-pixel magnitude ( $\beta$ ) and statistical significance ( $p$ -values) of the greening trends.

### 2.3 Mapping different land-use transitions

In our study area, we considered natural forests, oil palms, and croplands as the major land use types, as they together accounted  
for over 90% of the land cover. To delineate the annual changes of all these land use types from 2001 to 2016, we harmonized

95 various land use datasets, which were provided at different spatial resolutions (Table S1), into a unified dataset on a 500 m grid. This harmonization was essential to make land use changes across various datasets compatible with each other, and to match the spatial resolution of the land use data to LAI dataset. As shown in Fig. 1 and Fig. S1, the workflow for harmonizing multiple land cover datasets involved the following steps:

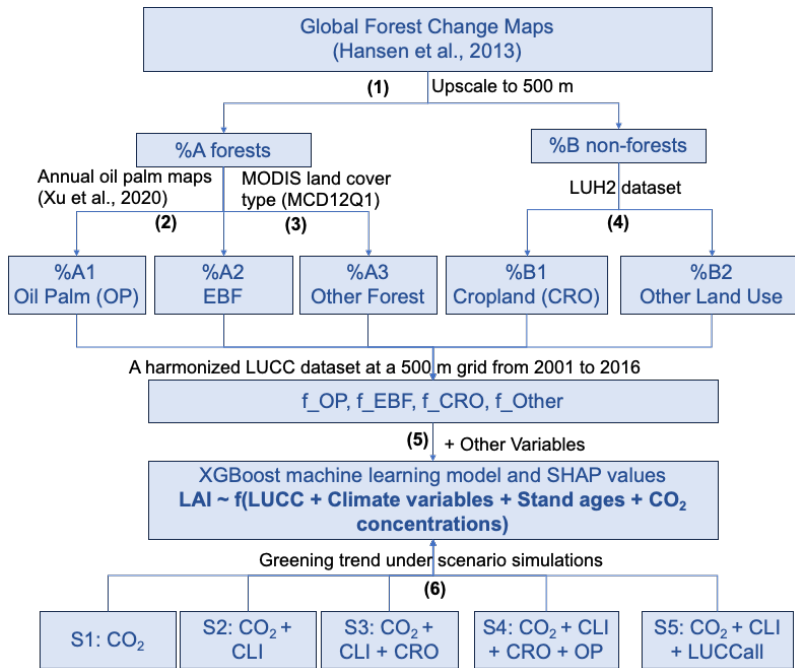
100 (1) We first determined the annual percentages of forested (A%) and non-forested areas (B%) within each 500 m grid cell by aggregating the mean of the annual 30 m resolution Global Forest Change v1.11 (GFC) maps (Hansen et al., 2013), using the *'reduceResolution()'* function in Google Earth Engine (<https://developers.google.com/earth-engine/guides/resample>).

(2) Within the forested fraction of each grid cell, we estimated the proportion of oil palm (OP) plantations (A1%) using an openly available dataset that covers OP distribution from 2001 to 2016 across Malaysia and Indonesia (Xu et al., 2020). To estimate the proportion of OP, we calculated the frequency of oil palm pixels in each 500 m × 500 m window.

105 (3) After accounting for the area of OP, the remaining forested area in each grid was further categorized into the evergreen broadleaf forest (EBF) (A2%) and other forest types (i.e., deciduous broadleaf forest, coniferous forest, mixed forest, etc.), based on the ratio of EBF to the total forested area provided by MODIS Land Cover Type Product (MCD12Q1 v6.1) (Sulla-Menashe and Friedl, 2018).

110 (4) Within the non-forested fraction of each grid cell, we used the latest version of the Land-use harmonization datasets (LUH2) dataset (Hurt et al., 2020) to estimate the percentage of cropland (CRO) (B1%) and other non-forest land uses (i.e., pasture, grass, etc.). In this analysis, we assumed that the fraction of each land use type in the LUH2 dataset on a 0.25° grid is applicable to the 500 m grid cells within each 0.25° grid cell. To avoid biases during downscaling land cover data from coarse to fine resolution, we also tested our results by upscaling all datasets to 0.25° (Fig. S2 and Fig. S3).

115 In the end, we obtained detailed information for EBF, OP, CRO, and Other (including other forests and non-forest vegetated areas) land-use types, at the 500 m spatial resolution. We grouped other forests and other non-forest vegetated areas together, as they represented a minor proportion (less than 5%) of the land surface (Table S2) and exhibited minimal changes during the study period.



120 **Figure 1: Workflow of the study. Steps (1) to (4) outline the processes for harmonizing multiple land cover datasets. Steps (5) to (6) show the establishment and interpretation of the LAI prediction and the process of scenario simulations.**

## 2.4 Extreme gradient boosting model

125 Tree-based machine learning models, such as Extreme Gradient Boosting (XGBoost), have been widely used in predicting and analysing ecosystem dynamics (Green et al., 2022; Yuan et al., 2019). Compared to neural networks, which often function like 'black boxes', tree-based models offer greater interpretability and are particularly effective on tabular-style datasets (Lundberg et al., 2020). XGBoost is an ensemble learning algorithm that iteratively constructs multiple decision trees and has proven to be effective for both classification and regression tasks (Yan et al., 2020; Chen and Guestrin, 2016). This algorithm employs shrinkage techniques and performs multithreaded calculations to minimize overfitting (Meng et al., 2021).

130 In our study, we applied the XGBoost algorithm (Chen and Guestrin, 2016) to model the spatial-temporal variations in the mean annual LAI using climatic and LUCC factors as inputs. These factors include the fractions of EBF, OP, CRO, and Other land uses, EBF-stand and OP-stand ages (Besnard et al., 2021; Danylo et al., 2021), CO<sub>2</sub> concentrations (<https://gml.noaa.gov/ccgg/trends/>), and climatic variables (Table S3). The climatic variables in our study include mean annual temperature (MAT), mean annual precipitation (MAP), wind speed (WS), shortwave radiation (RAD), and relative humidity (RH). These gridded climatic variables were obtained from the European Centre of Medium - Range Weather Forecasts (ECMWF) reanalysis product v5 - Land (<https://cds.climate.copernicus.eu/cdsapp#!/dataset/reanalysis-era5-land>). We aggregate the original hourly data to the annual time step using an annual average.

To fine-tune the parameters of our XGBoost model for LAI prediction, we randomly split the data into training and testing sets with a ratio of 80%:20%. We then utilized the GridSearchCV method to test different parameter combinations (i.e., varying numbers of trees from 150 to 400, tree depths from 5 to 15, and learning rates between 0.01 and 0.1) and determined the best parameter combinations through cross-validation (Pedregosa et al., 2011).

## 2.5 Shapley additive explanations

We utilized the TreeExplainer-based SHapley Additive exPlanations (SHAP) framework to interpret the individual and interactive contributions of LUCC and other factors (including climate variables, CO<sub>2</sub> concentration, and stand ages) to the LAI variations in our XGBoost model. The SHAP methodology, which is based on the concept of Shapley values in cooperative game theory, offers an insightful interpretation of factor importance (Lundberg and Lee, 2017). It provides detailed, instance-specific explanations, termed SHAP values to quantify the impact of each factor on the model predictions (Yang et al., 2021; Lundberg et al., 2020).

In the SHAP framework, the value for a given factor  $i$  in a particular sample  $x$  is computed as the average marginal contribution of that factor across all possible combinations. This is mathematically represented as:

$$\phi_i(x) = \sum_{S \subseteq N \setminus \{i\}} \frac{|S|! (|N| - |S| - 1)!}{|N|!} [f(S \cup \{i\}) - f(S)] \quad (1)$$

where  $N$  is the set of all factors,  $S$  is a subset of factors, and  $f$  is the prediction model. This formula quantifies the contribution of factor  $i$  by comparing the prediction with and without the factor, averaging over all possible subsets of factors.

The SHAP value indicates the magnitude and direction of the impact of a factor on prediction in the specific sample. To be specific, the magnitude (absolute value) of a SHAP value indicates the importance of a factor. Larger absolute SHAP values mean the factor has a greater impact on the model's output. The sign of a SHAP value (positive or negative) shows the direction of the impact. A positive SHAP value indicates that the factor positively affects the model's output (e.g., increases LAI), while a negative SHAP value suggests a negative impact (e.g., decreases LAI). By aggregating mean SHAP values of all samples, we can also derive global factor importance, which offers a holistic view of variables affecting annual LAI variations.

Furthermore, SHAP values aid in the interpretation of the interactive effects of two or more factors in machine learning models (Lundberg and Lee, 2017). The interactive effect is defined as the change in prediction when the joint contribution of two or more factors is considered, by subtracting the individual contributions made by each factor. The interactive effects of  $i^{\text{th}}$  and  $j^{\text{th}}$  factors are expressed as,

$$\phi_{i,j}(x) = \sum_{S \subseteq N \setminus \{i,j\}} \frac{|S|! (|N| - |S| - 2)!}{|N|!} [f(S \cup \{i,j\}) - f(S \cup \{i\}) - f(S \cup \{j\}) + f(S)] \quad (2)$$

We utilized the *xgboost* and *scikit-learn* packages in Python 3.11.0 for developing and training the XGBoost model (Chen and Guestrin, 2016; Pedregosa et al., 2011). Then, we employed the 'TreeExplainer' function from the *shap* (Lundberg and Lee, 2017) package to interpret the impact of factors on LAI predictions.

## 2.6 Simulation scenarios

To quantify and compare the impacts of specific LUCC processes, climate change, and elevated CO<sub>2</sub> concentrations on vegetation greenness changes, we adopted the scenario simulation framework from several factorial attribution analyses (Sitch et al., 2015). Specifically, we first estimated the LAI trend under five hypothetical scenarios (S1 to S5) using the established XGBoost model. The equations are as below,

$$LAI_{i,t,S_n} = XGBoost(CO2_{i,t,S_n}, CLI_{i,t,S_n}, f\_EBF_{i,t,S_n}, f\_CRO_{i,t,S_n}, f\_OP_{i,t,S_n}, f\_Other_{i,t,S_n}) \quad (3)$$

$$\beta LAI_{i,S_n} = slope(LAI_{i,S_n}) \quad (4)$$

Where,  $LAI_{i,t,S_n}$  represents the simulated LAI for the  $i^{\text{th}}$  grid at year of  $t$  under scenario  $S_n$ , and  $\beta LAI_{i,S_n}$  indicates the LAI trend over the study period. The *XGBoost* stands for the established model for LAI prediction using CO<sub>2</sub> concentration (CO<sub>2</sub>), climate variable (CLI), and land cover types such as fraction of evergreen broadleaf forest (f\_EBF), cropland (f\_CRO), oil palm (f\_OP), other land uses (f\_Other) (see Method 2.4).

For different scenarios, we adjusted the input variables according to specific assumptions to progressively incorporate different factors. For S1, we assumed only CO<sub>2</sub> concentration varied from 2001 to 2016, while climate and land use variables (i.e., CLI, f\_EBF, f\_CRO, f\_OP and f\_Other) remained constant at their values in 2001. For S2, CO<sub>2</sub> and climate change over time, with land uses remaining unchanged since 2001. S3 to S5 sequentially considered different land use processes. S3 involved changes from EBF to CRO using time-varying CO<sub>2</sub>, climate, and CRO fractions, while keeping OP and other land use types constant post-2001; S4 included conversions from EBF to both CRO and OP using time-varying CO<sub>2</sub>, climate, CRO and OP fractions, while other land uses unchanged since 2001; S5 encompassed all LUCC changes, with all variables including CO<sub>2</sub>, climate, and all types of LUCC varying over time.

We then quantified the impacts of each factor on vegetation greening based on differences in LAI trends between scenarios,

$$Driver_n = \delta LAI \text{ trend} = \beta LAI_{i,S_n} - \beta LAI_{i,S(n-1)} \quad (5)$$

Here,  $Driver_n$  measures the impact of the  $n^{\text{th}}$  driver (ranging from CO<sub>2</sub>, climate change, CRO expansion, OP expansion, to Other LUCC) on LAI trends. Notably,  $Driver_1$  quantifies the impact of CO<sub>2</sub>, equal to  $\beta LAI_{i,S_1}$ . In addition, our estimation of CRO or OP expansion assumed that the increased areas of CRO or OP since 2001 came from EBF, given CRO and OP expansion mostly resulted from deforestation in Indonesia and Malaysia (Numata et al., 2022; Wagner et al., 2022).

## 3. Results

### 3.1 Land use changes and greening trends

From 2001 to 2016, the extent of forest in our study area decreased annually by 1.29%, leading to a reduction in EBF from 73.41% to 53.09% of the study area. Notably, approximately 25.54% of the region experienced rapid deforestation with a

forest loss rate exceeding 2% of the land surface per year. This deforestation rate was especially pronounced in the eastern parts of Sumatra and along the western and southern edges of Borneo (Fig. 2b).  
200

In the deforested areas, we observed widespread expansions of CRO and OP plantations. The area of CRO increased at a rate of 0.63% per year, resulting in an increase of CRO from 14.45% to 24.56% of the region (i.e.,  $20.76 \times 10^4 \text{ km}^2$  to  $35.28 \times 10^4 \text{ km}^2$ ) from 2000 to 2016. Meanwhile, the expansion of OP proceeded at a pace of 0.48% per year, resulting in nearly tripled the extent of oil plantations over the past decade (i.e., from 3.91% in 2001 to 12.05% in 2016; Fig. 2a). In central Sumatra, the  
205 south edge of Borneo, and the southern part of Peninsula Malaysia, OP showed the largest increase, partly at the expense of decreases in CRO (Fig. 2c).

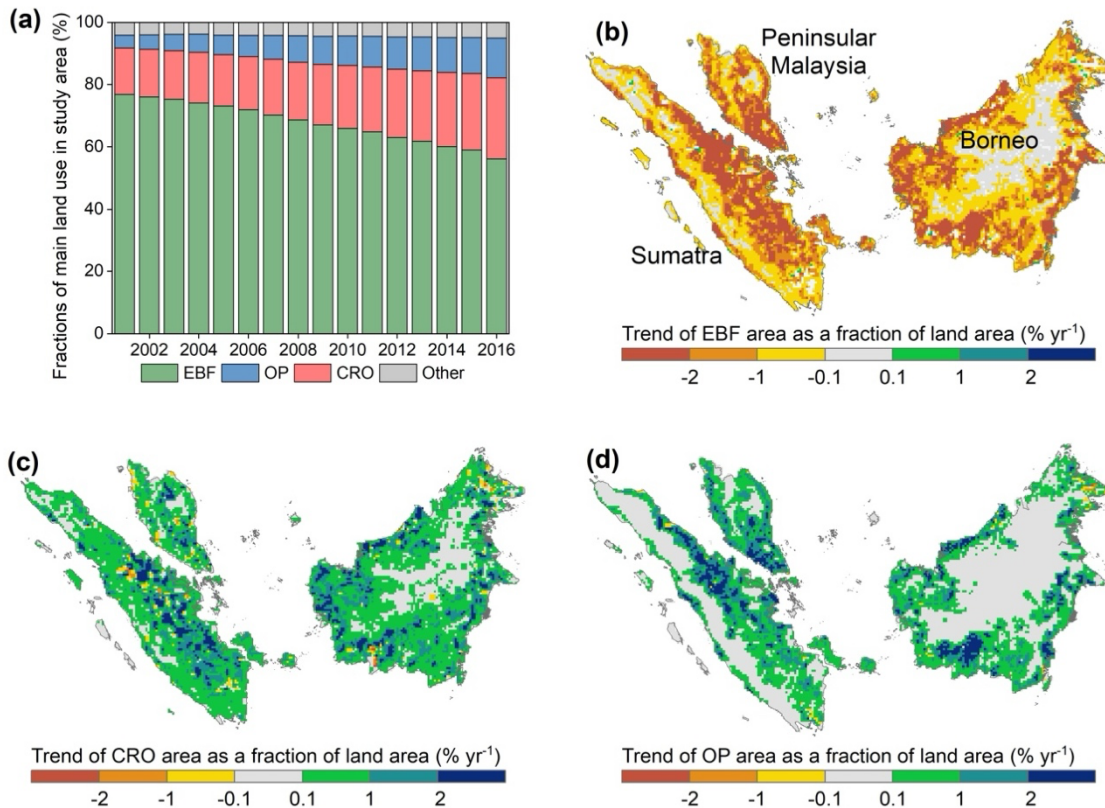
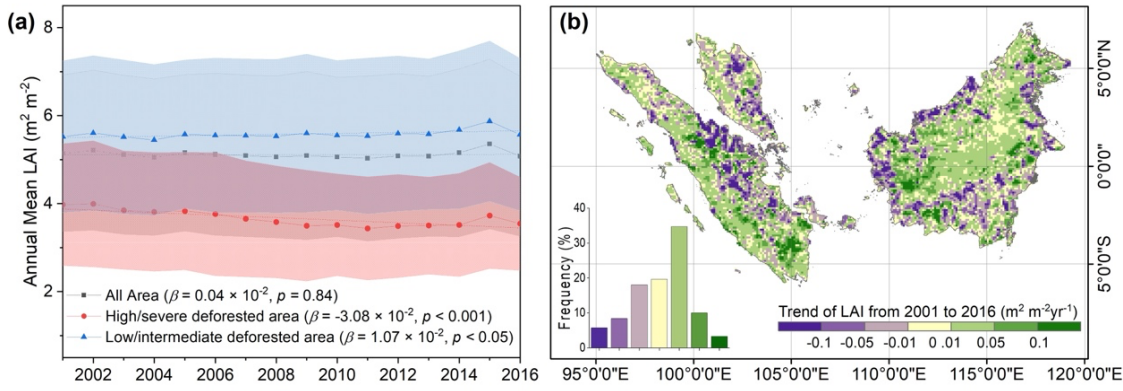


**Figure 2: Land use composition and its changes from 2001 to 2016 in the study area. (a) The changes in the fractions of main land uses including evergreen broadleaf forest (EBF), oil palm (OP), cropland (CRO), and others over the study period. (b)-(d) Spatial distribution of the trend of EBF, CRO, and OP as a fraction of land area.**  
210

The regional average LAI exhibited a non-significant upward trend over the study period, with a slope of  $0.04 \times 10^{-2} \text{ m}^2 \text{ m}^{-2} \text{ yr}^{-1}$  (Fig. 3a). Using another LAI dataset (MODIS LAI), we also captured the increasing trend (Fig. S4). According to Galán-Acedo et al. (2021), areas with over 70% forest loss are categorized as having high to severe deforestation, while areas with less than 70% forest loss are classified as undergoing low to intermediate deforestation. We found that for our study area, the

215 non-significant upward trend in LAI was due to a net effect of a rapid LAI increase ( $\beta = +1.07 \times 10^{-2} \text{ m}^2 \text{ m}^{-2} \text{ yr}^{-1}$ ,  $p < 0.05$ ) in areas with low to intermediate deforestation and a significant LAI decline ( $\beta = -3.08 \times 10^{-2} \text{ m}^2 \text{ m}^{-2} \text{ yr}^{-1}$ ,  $p < 0.001$ ) in areas with high to severe deforestation (Fig. 3a). Across the study area, 58.50% of the region showed a significant decreasing LAI trend and they are mostly areas with pronounced forest loss (Fig. 3b and Fig. 2b).



220 **Figure 3: The trends of LAI from 2001 to 2016 in the study area. (a) Regional average LAI trend, the LAI trends from regions with high to severe deforestation, and LAI trend from regions with low to intermediate deforestation. The classification of the deforestation level is referred to Galán-Acedo et al. (2021), where areas experiencing more than 70% forest loss are classified as high/severe deforestation, whereas those with less than 70% loss are classified as low/intermediate deforestation. (b) the spatial pattern of LAI trend, with histogram plot showing the frequency (%) of the pixel-wise LAI trend in the study area.**

### 225 3.2 Drivers of changes in LAI

To understand the variations in vegetation greenness in Southeast Asia, we established an XGBoost model to quantify the relationship between vegetation greenness and land uses, climate variables, CO<sub>2</sub> concentrations, and stand ages. The XGBoost model showed high explanatory power (i.e., 98% accuracy for calibration and 93% accuracy for validation), underscoring the model's reliability for analysing the determinants of LAI variability (Fig. 4). Using different splitting ratios for calibration and validation dataset, we obtained the similar model performance (Fig. S5).

230

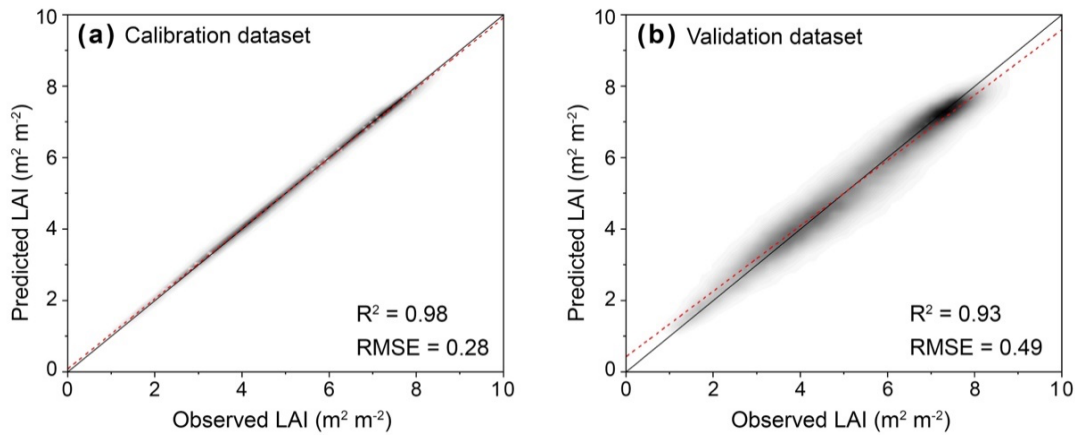


**Figure 4: Comparison of observed and predicted LAI values with the XGBoost model for the calibration dataset (a) and validation dataset (b).**

Based on the built XGBoost model, we evaluated the contributions of each factor to LAI in the SHAP framework (Fig. 5; see  
 235 Methods). Our results revealed that the fraction of EBF ( $f_{\text{EBF}}$ ) in each grid holds the greatest mean absolute SHAP value (1.28), indicating that  $f_{\text{EBF}}$  had the largest impact on LAI (Fig. 5b) and this impact was positive (Fig. 5a and Fig. S6a).

The average impact of the fraction of OP ( $f_{\text{OP}}$ ) on LAI ranked the second largest (0.21) and had a similar positive impact on  
 LAI as  $f_{\text{EBF}}$  (Fig. 5a, b and S6b). In contrast, the impact of CRO and other land uses on LAI was found to be negative (Fig.  
 5a, S6c and S6d). A higher fraction of CRO ( $f_{\text{CRO}}$ ) led to a larger negative SHAP value. We further explored the impacts of  
 240 interactions of land use types (i.e.,  $f_{\text{CRO}}$ ,  $f_{\text{OP}}$  and  $f_{\text{EBF}}$ ) on LAI. The results demonstrated that in areas with low  $f_{\text{EBF}}$ ,  
 an increase of  $f_{\text{OP}}$  enhanced LAI while  $f_{\text{CRO}}$  induced LAI decreases. Meanwhile, in areas with high  $f_{\text{EBF}}$ , the impacts  
 of both  $f_{\text{OP}}$  and  $f_{\text{CRO}}$  on LAI are markedly reduced, suggesting dominant role of  $f_{\text{EBF}}$  on greenness in the region (Fig.  
 5c and 5d).

Apart from the impacts of land uses on LAI, we also found that elevated CO<sub>2</sub> concentration substantially increased LAI, with  
 245 a mean SHAP value of 0.18. In contrast to elevated CO<sub>2</sub> concentration, the MAT was negatively related to LAI with a smaller  
 mean SHAP value of 0.08 (Fig. 5b and S6e). Other climate variables have limited impacts on LAI. It is noteworthy is that the  
 stand ages of both EBF ( $\text{Age}_{\text{EBF}}$ ) and stand ages of OP ( $\text{Age}_{\text{OP}}$ ) positively impact LAI. Specifically,  $\text{Age}_{\text{EBF}}$  has a  
 greater impact than that of  $\text{Age}_{\text{OP}}$ , as indicated by a higher absolute mean SHAP value for  $\text{Age}_{\text{EBF}}$  (0.11) compared to  
 $\text{Age}_{\text{OP}}$  (0.08). While we found that  $\text{Age}_{\text{EBF}}$  continuously contributed to LAI increases (Fig. S6k),  $\text{Age}_{\text{OP}}$  increased LAI  
 250 at a younger age (less than 12 years) and then decreased LAI afterward (Fig. S6l).

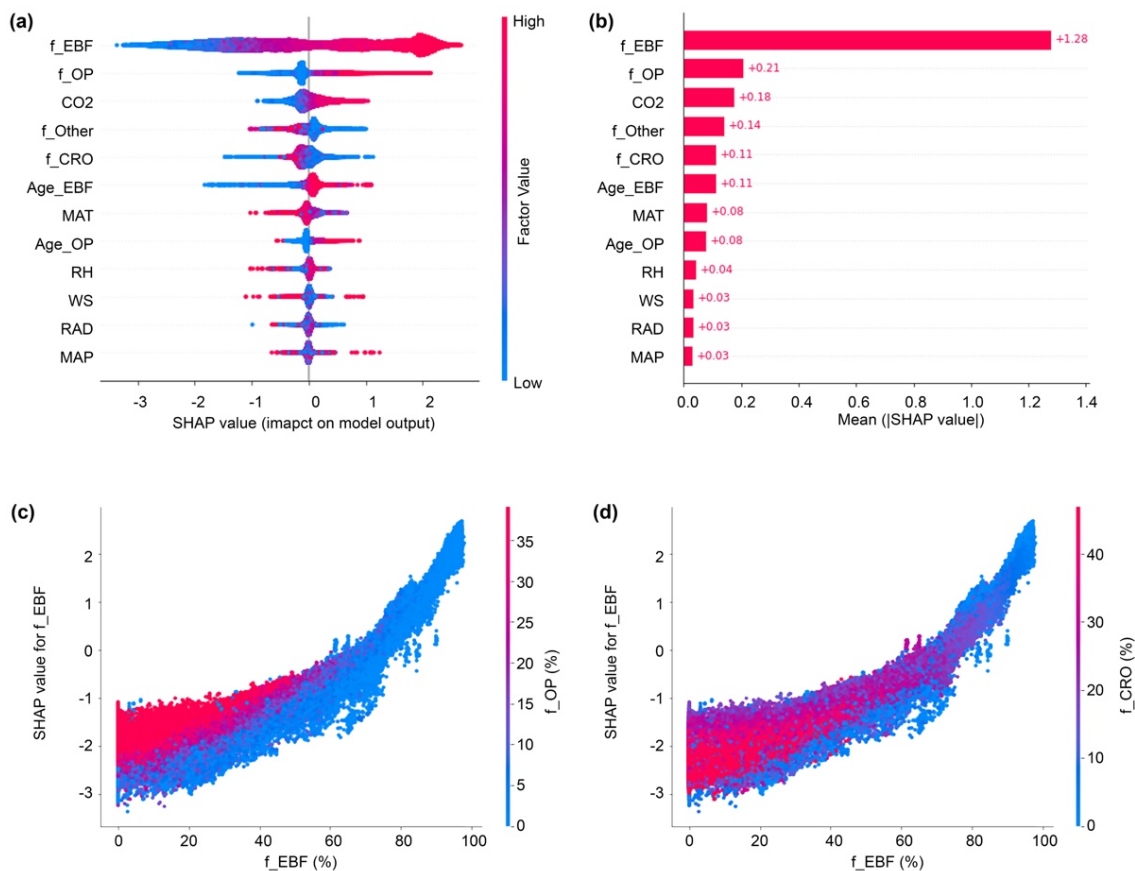


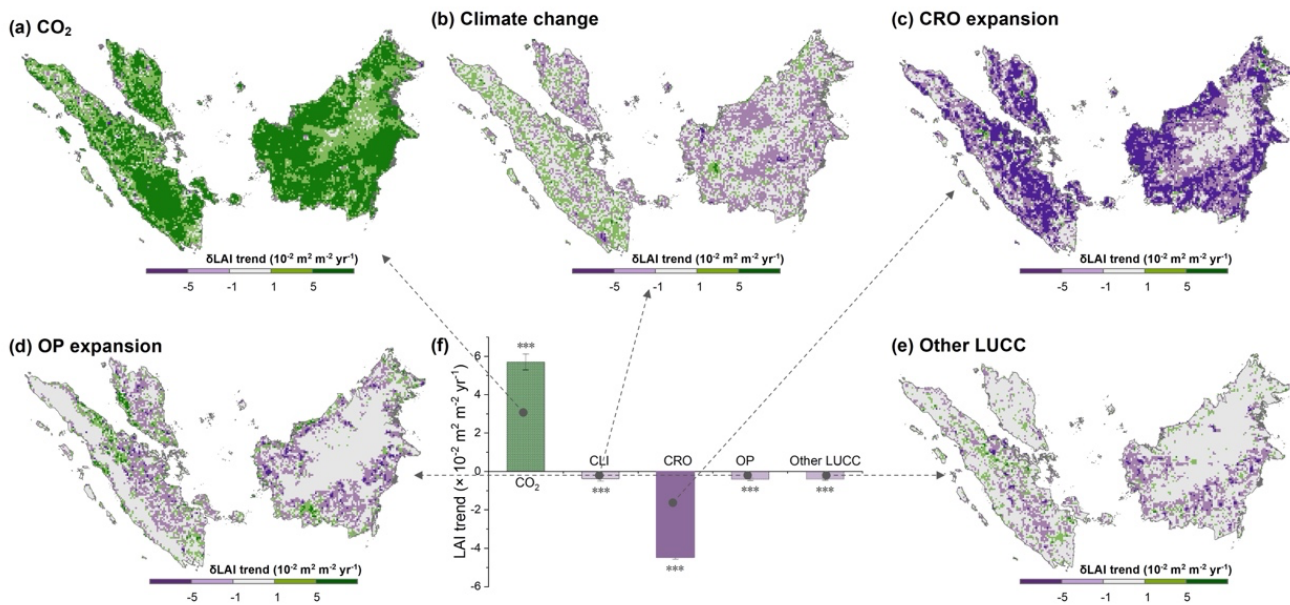
**Figure 5: The impact of factors on LAI. (a) Beeswarm plots show the SHAP values of each factor on LAI for each sample. The SHAP value indicates the magnitude and direction of the impact on LAI (see Methods). Each dot represents an individual sample, with the color indicating the relative values of the specific factor. (b) The bar plot of the mean absolute SHAP values of each factor for LAI. (c) The interaction of f\_OP and f\_EBF, and (d) the interaction of f\_CRO and f\_EBF on LAI. The abbreviations for each factor are available in Table S3.**

### 3.3 Impacts of LUCC on greening

Through scenario-based prediction, we quantified the impacts of LUCC, elevated CO<sub>2</sub> concentration and climate change on the trend of greening (Fig. 6f and Fig. S8). Compared to the observed greening trend for the study area (i.e.,  $0.04 \times 10^{-2} \text{ m}^2 \text{ m}^{-2} \text{ yr}^{-1}$ ), we found that the greening trend increased to  $5.71 \times 10^{-2} \text{ m}^2 \text{ m}^{-2} \text{ yr}^{-1}$  under the scenario S1, which simulated the effect of elevated CO<sub>2</sub> alone with climate and LUCC remaining constant. The result suggests that elevated CO<sub>2</sub> was the primary reason for the increase of LAI in Southeast Asia if there were. Climate change showed a small negative impact (i.e., mostly due to rising temperature) on the LAI. We found both CRO expansion and OP expansion decreased LAI trend, with the trend dramatically dropping by  $-4.46 \times 10^{-2} \text{ m}^2 \text{ m}^{-2} \text{ yr}^{-1}$  under the impact of CRO expansion, and by  $-0.41 \times 10^{-2} \text{ m}^2 \text{ m}^{-2} \text{ yr}^{-1}$  under the impact of OP expansion. The results highlight that CRO expansion was the primary reason for the decrease in vegetation

greenness, counteracting the greening trend caused by elevated CO<sub>2</sub> in our study area. In contrast, OP expansion only contributed to a small decline in greenness.

We further examined the spatial variations of the impacts of each factor on greening by quantifying the differences in greening trends under different scenarios at the pixel level. Across the study area, LUCC imposed a negative impact on LAI trends (Fig. 270 6c, 6d, and 6e). Consistent with regional average values, we found the changes from EBF to CRO had a more pronounced negative impact on the greening trend than the conversion of EBF to OP (Fig. 6c and 6d). In some regions, such as the southern edges of Sumatra and Borneo, OP enhanced regional greening (Fig. 6d). Meanwhile, elevated CO<sub>2</sub> concentrations consistently had a positive impact on greening across the region (Fig. 6a), and climate change showed an overall negative but highly heterogeneous impact on LAI trends (Fig. 6b). From a spatial perspective, we found that elevated CO<sub>2</sub> dominated the increase in LAI in most areas, accounting for 62.10% of the study area, while CRO expansion was the primary driver in LAI decrease in other regions (26.33%), especially coastal areas (Fig. S7). 275



280 **Figure 6: The spatial distribution of the pixel-wise impacts of each factor on the greening trends ( $\delta$ LAI trend). Positive values mean the factors considered increase LAI trend, and negative values mean otherwise. We show the spatial patterns of contribution from (a) elevated CO<sub>2</sub> concentrations, (b) climate changes, (c) expansion of cropland (CRO), (d) expansion of oil palm (OP), and (e) other land use changes. (f) shows the average impact of each factor, with the error bars indicating one standard deviation. The symbol (\*\*\*) denotes a statistically significant difference in LAI trends at  $p < 0.001$  level.**

#### 4. Discussion

In this study, we analysed the typical LUCC processes in Peninsular Malaysia, Sumatra and Borneo and their impacts on greenness over the past two decades. We found a significant decline in EBF coverage, from 73.41% to 53.09%, predominantly 285 due to CRO and OP plantation expansions. Meanwhile, we did not find a significant trend in LAI in our study area, as the

increases in regional greenness due to elevated CO<sub>2</sub> were offset by the decreases in regional greenness caused by CRO and OP expansions. Notably, the negative effect of CRO expansion ( $-4.46 \times 10^{-2} \text{ m}^2 \text{ m}^{-2} \text{ yr}^{-1}$ ) was more pronounced than that of OP expansion ( $-0.41 \times 10^{-2} \text{ m}^2 \text{ m}^{-2} \text{ yr}^{-1}$ ), indicating a dominant role of CRO expansion on greenness decline in our study area.

#### 290 **4.1 Strong negative impact of cropland expansion on greenness in Southeast Asia**

Our results demonstrate that CRO expansion in Southeast Asia contributed negatively to vegetation greenness. This is opposite to reports on the greening trend in China and India, where CRO are suggested as the main reason for the net increase in LAI (Kuttippurath and Kashyap, 2023; Chen et al., 2019). This disparity may be partly attributed to original land use types before CRO expansion. In Southeast Asia, CRO expansion mainly occurs at the expense of natural forests (Potapov et al., 2022; Zeng  
295 et al., 2018), and crops often have less dense canopies than natural forests (Pocock et al., 2010; Foley et al., 2005; Asner et al., 2005). In contrast, the increase in LAI in China and India primarily resulted from the intensification of croplands, rather than their expansion, and where expansion did occur, it predominantly took place on lands that were previously bare or sparsely vegetated (Chen et al., 2019).

We also note that agricultural practices in Indonesia and Malaysia are generally less intensive compared to India and China,  
300 partly due to less advanced agricultural technologies deployed in the region (Liu et al., 2021). For example, in China and India, intensive agricultural practices, including precision fertilization and advanced irrigation systems, such as drip irrigation in China and spray irrigation in India, are widely adopted to enhance crop growth (Cui et al., 2022; Wang et al., 2013). In addition, the development of specialized crop varieties, such as hybrid rice in China and climate-smart drought-tolerant rice varieties in India (Zhang et al., 2022; Panda et al., 2021), also facilitated plant growth and, consequently, regional greening (Zhao et al.,  
305 2023; Zhao et al., 2021). In contrast, Indonesia and Malaysia predominantly depend on rainfed irrigation and traditional farming methods, such as the Subak terraced rice fields in Indonesia, leading to lower crop intensity. Less intensive practices are less likely to create dense canopy and biomass of croplands (Takeshima, 2019).

#### **4.2 Minor contribution of oil palm to regional greenness**

Our study observed a negative, yet small impact of OP expansion on greenness. This aligns with studies reporting that OP has  
310 LAI values comparable to, or only slightly lower than, native forests (Rusli and Majid, 2014; Propastin, 2009; Vernimmen et al., 2007). Therefore, OP expansion, though a major driver for land use change in Southeast Asia, was not a main driver of greenness decline in the region.

Meanwhile, we also found that the age of OP stands influences LAI, as the LAI of OP increases stand age when OP is young, and then decreases LAI after a threshold of stand age. This observation agrees with previous studies reporting the plateau and  
315 decrease of oil palm LAI after the age of 10 (Xu et al., 2021), and the plateau and decrease of oil palm yield after the age of 8-9 (Park et al., 2023). The stand age of most OP planted in Southeast Asia is approaching maturity (over half were planted before 2009) (Danylo et al., 2021). In response, industrial and smallholder plantations have undergone or are starting to undergo the process of replanting (Numata et al., 2022; Danylo et al., 2021) although replanting in smallholder plantations is

often delayed as farmers face more financial constraints (Zhao et al., 2023). Hence, we expect to see a more complex influence  
320 of OP on LAI trend depending on the management practices of different types of plantations.

In comparison with CRO, our findings indicate that the impact of OP expansion on vegetation greenness decline is relatively  
minor (Fig. 6). This can be attributed to the generally higher biomass of OP compared to typical crops like rice and maize in  
Indonesia and Malaysia. In addition, we assumed CRO or OP expansion that the increased areas of CRO or OP since 2001  
325 came from EBF in our study. While CRO and OP expansion indeed mostly resulted from deforestation in Indonesia and  
Malaysia (Numata et al., 2022; Wagner et al., 2022), the expansions of CRO and OP can also come from other land uses (i.e.,  
grasslands or pastures). Transitions from these land uses to CRO and OP might result in a smaller negative impact on vegetation  
greenness, we suspect, considering grasslands and shrubs have smaller LAI than EBF.

### **4.3 Other LUCC impacts on greenness in Southeast Asia**

While our study examined the two most prominent processes of LUCC in Southeast Asia (EBF to OP and EBF to CRO), there  
330 are other types of land use changes we analysed together under the category of “Other” land use types. The changes in these  
land use types are also relevant to deforestation, and they include other plantations such as rubber plantations (Wang et al.,  
2023b), agroforests such as cocoa and coffee (Panda et al., 2021), and grasslands or pastures (Austin et al., 2019). In total,  
“Other” accounted for 4.70% of the study area in 2016, much less than the three main types we studied (51.06% for EBF,  
25.01% for CRO, and 12.09% for OP in 2016), and experienced minor changes since 2001.

335 Meanwhile, we found the overall impact of these other LUCC on greenness was likely small (Fig. 6f). The small impact is  
contingent on their smaller extent compared to EBF, CRO and OP (see above). It may also result from the offset of positive  
and negative impacts from individual Other LUCC processes on greenness. For example, rubber plantations exhibit a higher  
LAI than natural forests (Wang et al., 2022), while agroforestry and other plantations generally have a lower LAI than natural  
forests, therefore leading to different trends in LAI after deforestation.

### **4.4 Impact of climate change and CO<sub>2</sub> concentrations on regional greenness**

CO<sub>2</sub> fertilization effects appear to be the primary drivers of greening trends observed in global studies (Chen et al., 2022; Zhu  
et al., 2016; Ewert, 2004). Our research also confirmed the substantial contribution of rising CO<sub>2</sub> levels to the greening of  
vegetation in Southeast Asia. The impact of temperature on greenness in Southeast Asia was negative, in contrast to the positive  
effects noted in cold climate zones, such as the Qinghai-Tibet Plateau (Yang et al., 2024; Zhao et al., 2023b; Zhong et al.,  
345 2019) and Arctic areas (Forbes et al., 2010). We suspect that the negative effect of temperature implies that temperature may  
have exceeded the optimal point for plant growth in parts of Southeast Asia. This aligns with several studies suggesting that  
ecosystem functions in the tropics are approaching a temperature tipping point (Doughty et al., 2023; Wu et al., 2019; Meir et  
al., 2015). Additionally, temperature rise might exacerbate the incidence of pests and diseases in tropical forests, negatively  
impacting plant health and productivity (Ghini et al., 2011). These factors might contribute jointly to the observed decline in  
350 greenness with increasing temperatures in Southeast Asia.

## 5. Conclusion

Our study closely examined the impacts of LUCC on vegetation greenness in part of Southeast Asia. We found that there was no significant trend in vegetation greenness in the study area, which is attributed to the net effect of negative impacts of LUCC on LAI and positive influence of elevated CO<sub>2</sub> on LAI. Among various LUCC processes, we found that cropland expansion  
355 was the primary reason for LAI decrease, while oil palm expansion had a small impact on LAI trends. These results shed light on the interplay between greenness and land use changes and provide valuable insight into our future studies on terrestrial carbon, water, and energy budgets in the land use change-intensive Southeast Asia.

## Acknowledgment

XL and RZ are supported by a Tier 2 research grant from Singapore Ministry of Education (A-8001551-00-00) and a Singapore  
360 Energy Centre Core project (A-8000179-00-00). We also thank Tin Widyani Satriawan, a PhD student in our group, for her valuable suggestions on refining the manuscript's language.

## Data Availability

The GLOBMAP LAI dataset is obtained from <https://zenodo.org/records/4700264>. Climatic variables, including temperature, precipitation, wind speed, shortwave downward radiation, and humidity, were obtained from the ERA5 model  
365 (<https://cds.climate.copernicus.eu/cdsapp#!/dataset/reanalysis-era5-single-levels?tab=form>). The distribution of forest age and plantation age maps was obtained from the (<https://sedac.ciesin.columbia.edu/data/collection/gpw-v4>). CO<sub>2</sub> concentrations are obtained from (<https://gml.noaa.gov/dv/data/>).

## Code Availability

The code used for this research will be made publicly available upon acceptance of the manuscript.

## 370 Author contribution

XL and RZ conceptualized the study, visualization, and writing of the original draft preparation. RZ and YY contributed to the data curation, methodology, and software development. RZ, XL, and YY performed the formal analysis. XL acquired the funds. LS, CC and JL were behind the project administration and the supervision of the research planning. RZ and YY contributed to the software development. All authors contributed to the writing review, editing, and validation.

## 375 Competing interest

The authors declare no competing interests.

## Reference

- Asner, G. P., Knapp, D. E., Broadbent, E. N., Oliveira, P. J. C., Keller, M., & Silva, J. N. (2005). Selective Logging in the Brazilian Amazon. *Science*, *310*(5747), 480-482. <http://doi.org/10.1126/science.1118051>
- 380 Austin, K. G., Schwantes, A., Gu, Y., & Kasibhatla, P. S. (2019). What causes deforestation in Indonesia? *Environmental Research Letters*, *14*(2), 24007. <http://doi.org/10.1088/1748-9326/aaf6db>
- Besnard, S., Koiralala, S., Santoro, M., Weber, U., Nelson, J., & Günter, J., et al. (2021). Mapping global forest age from forest inventories, biomass and climate data. *Earth System Science Data*, *13*(10), 4881-4896. <http://doi.org/10.5194/essd-13-4881-2021>
- 385 Chen, C., Park, T., Wang, X., Piao, S., Xu, B., & Chaturvedi, R. K., et al. (2019). China and India lead in greening of the world through land-use management. *Nature Sustainability*, *2*(2), 122-129. <http://doi.org/10.1038/s41893-019-0220-7>
- Chen, C., Riley, W. J., Prentice, I. C., & Keenan, T. F. (2022). CO<sub>2</sub> fertilization of terrestrial photosynthesis inferred from site to global scales. *Proceedings of the National Academy of Sciences*, *119*(10). <http://doi.org/10.1073/pnas.2115627119>
- 390 Chen, J. M., & Black, T. A. (1992). Defining leaf area index for non-flat leaves. *Plant, cell and environment*, *15*(4), 421-429. <http://doi.org/10.1111/j.1365-3040.1992.tb00992.x>
- Chen, S., Woodcock, C., Dong, L., Tarrío, K., Mohammadi, D., & Olofsson, P. (2024). Review of drivers of forest degradation and deforestation in Southeast Asia. *Remote Sensing Applications: Society and Environment*, *33*, 101129. <http://doi.org/https://doi.org/10.1016/j.rsase.2023.101129>
- 395 Chen, T., & Guestrin, C. (2016), XGBoost: A Scalable Tree Boosting System, ACM, Ithaca, 2016-01-01.
- Chini, L., Hurtt, G., Sahajpal, R., Froking, S., Klein Goldewijk, K., & Sitch, S., et al. (2021). Land-use harmonization datasets for annual global carbon budgets. *Earth System Science Data*, *13*(8), 4175-4189. <http://doi.org/10.5194/essd-13-4175-2021>
- Cui, M., Qian, J., & Cui, L. (2022). Developing precision agriculture through creating information processing capability in rural China. *Journal of Rural Studies*, *92*, 237-252. <http://doi.org/10.1016/j.jrurstud.2022.04.002>
- 400 Danylo, O., Pirker, J., Lemoine, G., Ceccherini, G., See, L., & McCallum, I., et al. (2021). A map of the extent and year of detection of oil palm plantations in Indonesia, Malaysia and Thailand. *Scientific Data*, *8*(1), 96. <http://doi.org/10.1038/s41597-021-00867-1>
- Descals, A., Wich, S., Meijaard, E., Gaveau, D. L. A., Peedell, S., & Szantoi, Z. (2021). High-resolution global map of smallholder and industrial closed-canopy oil palm plantations. *Earth System Science Data*, *13*(3), 1211-1231. <http://doi.org/10.5194/essd-13-1211-2021>
- 405 Euler, M., Schwarze, S., Siregar, H., & Qaim, M. (2016). Oil Palm Expansion among Smallholder Farmers in Sumatra, Indonesia. *Journal of Agricultural Economics*, *67*(3), 658-676. <http://doi.org/https://doi.org/10.1111/1477-9552.12163>
- 410 Ewert, F. (2004). Modelling Plant Responses to Elevated CO<sub>2</sub>: How Important is Leaf Area Index? *Annals of Botany*, *93*(6), 619-627. <http://doi.org/10.1093/aob/mch101>
- Fagan, M. E., Kim, D., Settle, W., Ferry, L., Drew, J., & Carlson, H., et al. (2022). The expansion of tree plantations across tropical biomes. *Nature Sustainability*, *5*(8), 681-688. <http://doi.org/10.1038/s41893-022-00904-w>
- Fang, H., Baret, F., Plummer, S., & Schaepman Strub, G. (2019). An Overview of Global Leaf Area Index (LAI): Methods, Products, Validation, and Applications. *Reviews of Geophysics*, *57*(3), 739-799. <http://doi.org/10.1029/2018RG000608>
- 415 FAOSTAT (2022)., edited.
- Felbab-Brown, V. (2013), *An Atlas of Trafficking in Southeast Asia: the jagged edge: Illegal logging in Southeast Asia*, 113-136 pp., IB Tauris & Co. Ltd. New York.
- 420 Foley, J. A., DeFries, R., Asner, G. P., Barford, C., Bonan, G., & Carpenter, S. R., et al. (2005). Global Consequences of

- Land Use. *Science*, 309(5734), 570-574. <http://doi.org/10.1126/science.1111772>
- Forbes, B. C., Fauria, M. M., & Zetterberg, P. (2010). Russian Arctic warming and 'greening' are closely tracked by tundra shrub willows. *Global Change Biology*, 16(5), 1542-1554. <http://doi.org/10.1111/j.1365-2486.2009.02047.x>
- 425 Galán-Acedo, C., Spaan, D., Bicca-Marques, J. C., de Azevedo, R. B., Villalobos, F., & Rosete-Vergés, F. (2021). Regional deforestation drives the impact of forest cover and matrix quality on primate species richness. *Biological Conservation*, 263, 109338. <http://doi.org/10.1016/j.biocon.2021.109338>
- Geist, H. J., & F, L. E. (2001). What Drives Tropical Deforestation. *LUCC Report series*, 4, 116
- Ghini, R., Bettiol, W., & Hamada, E. (2011). Diseases in tropical and plantation crops as affected by climate changes: current knowledge and perspectives. *Plant Pathology*, 60(1), 122-132. <http://doi.org/10.1111/j.1365-3059.2010.02403.x>
- 430 Green, J. K., Ballantyne, A., Abramoff, R., Gentine, P., Makowski, D., & Ciais, P. (2022). Surface temperatures reveal the patterns of vegetation water stress and their environmental drivers across the tropical Americas. *Global Change Biology*, 28(9), 2940-2955. <http://doi.org/10.1111/gcb.16139>
- Hansen, M. C., Potapov, P. V., Moore, R., Hancher, M., Turubanova, S. A., & Tyukavina, A., et al. (2013). High-Resolution Global Maps of 21st-Century Forest Cover Change. *Science*, 342(6160), 850-853.
- 435 <http://doi.org/10.1126/science.1244693>
- Harris, N. L., Brown, S., Hagen, S. C., Saatchi, S. S., Petrova, S., & Salas, W., et al. (2012). Baseline map of carbon emissions from deforestation in tropical regions. *Science*, 336(6088), 1573-1576. <http://doi.org/10.1126/science.1217962>
- Houghton, R. A., & Nassikas, A. A. (2017). Global and regional fluxes of carbon from land use and land cover change 1850–2015. *Global Biogeochemical Cycles*, 31(3), 456-472. <http://doi.org/10.1002/2016GB005546>
- 440 Hurtt, G. C., Chini, L., Sahajpal, R., Froking, S., Bodirsky, B. L., & Calvin, K., et al. (2020). Harmonization of global land-use change and management for the period 850–2100 (LUH2) for CMIP6. *Geoscientific Model Development Discussions*, 2020, 1-65
- Ito, A., & Hajima, T. (2020). Biogeophysical and biogeochemical impacts of land-use change simulated by MIROC-ES2L. *Progress in Earth and Planetary Science*, 7(1). <http://doi.org/10.1186/s40645-020-00372-w>
- 445 Koh, L. P., & Wilcove, D. S. (2008). Is oil palm agriculture really destroying tropical biodiversity? *Conservation Letters*, 1(2), 60-64. <http://doi.org/10.1111/j.1755-263X.2008.00011.x>
- Kuttippurath, J., & Kashyap, R. (2023). Greening of India: Forests or Croplands? *Applied Geography*, 161, 103115. <http://doi.org/10.1016/j.apgeog.2023.103115>
- 450 Liu, X., Zheng, J., Yu, L., Hao, P., Chen, B., & Xin, Q., et al. (2021). Annual dynamic dataset of global cropping intensity from 2001 to 2019. *Scientific Data*, 8(1), 283. <http://doi.org/10.1038/s41597-021-01065-9>
- Liu, Y., Liu, R., & Chen, J. M. (2012). Retrospective retrieval of long-term consistent global leaf area index (1981-2011) from combined AVHRR and MODIS data. *Journal of Geophysical Research: Biogeosciences*, 117(G4), n/a-n/a. <http://doi.org/10.1029/2012JG002084>
- 455 Lundberg, M., & Lee, S. (2017). A Unified Approach to Interpreting Model Predictions. in *Advances in neural information processing systems*, edited.
- Lundberg, S. M., Erion, G., Chen, H., DeGrave, A., Prutkin, J. M., & Nair, B., et al. (2020). From local explanations to global understanding with explainable AI for trees. *Nature Machine Intelligence*, 2(1), 56-67. <http://doi.org/10.1038/s42256-019-0138-9>
- 460 Mann, H. B. (1945). Nonparametric Tests Against Trend. *Econometrica*, 13(3), 245. <http://doi.org/10.2307/1907187>
- Mao, F., Li, X., Zhou, G., Huang, Z., Xu, Y., & Chen, Q., et al. (2023). Land use and cover in subtropical East Asia and Southeast Asia from 1700 to 2018. *Global and Planetary Change*, 226, 104157. <http://doi.org/10.1016/j.gloplacha.2023.104157>
- Meng, Y., Yang, N., Qian, Z., & Zhang, G. (2021). What Makes an Online Review More Helpful: An Interpretation Framework Using XGBoost and SHAP Values. *Journal of Theoretical and Applied Electronic Commerce Research*, 16(3), 466-490. <http://doi.org/10.3390/jtaer16030029>
- 465 Miettinen, J., Shi, C., & Liew, S. C. (2011). Deforestation rates in insular Southeast Asia between 2000 and 2010. *Global Change Biology*, 17(7), 2261-2270. <http://doi.org/10.1111/j.1365-2486.2011.02398.x>
- Numata, I., Elmore, A. J., Cochrane, M. A., Wang, C., Zhao, J., & Zhang, X. (2022). Deforestation, plantation-related land cover dynamics and oil palm age-structure change during 1990–2020 in Riau Province, Indonesia. *Environmental*
- 470

- Research Letters*, 17(9), 94024. <http://doi.org/10.1088/1748-9326/ac8a61>
- Panda, D., Mishra, S. S., & Behera, P. K. (2021). Drought Tolerance in Rice: Focus on Recent Mechanisms and Approaches. *Rice Science*, 28(2), 119-132. <http://doi.org/10.1016/j.rsci.2021.01.002>
- 475 Park, T., Gumma, M. K., Wang, W., Panjala, P., Dubey, S. K., & Nemani, R. R. (2023). Greening of human-dominated ecosystems in India. *Communications Earth & Environment*, 4(1). <http://doi.org/10.1038/s43247-023-01078-9>
- Pedregosa, F., G., V., & Gramfort. (2011). Scikit-learn: Machine learning in Python. *Journal of Machine Learning Research*(12), 2825-2830
- Piao, S., Wang, X., Park, T., Chen, C., Lian, X., & He, Y., et al. (2020a). Characteristics, drivers and feedbacks of global greening. *Nature Reviews Earth & Environment*, 1(1), 14-27. <http://doi.org/10.1038/s43017-019-0001-x>
- 480 Piao, S., Wang, X., Park, T., Chen, C., Lian, X., & He, Y., et al. (2020b). Characteristics, drivers and feedbacks of global greening. *Nature reviews. Earth & environment*, 1(1), 14-27. <http://doi.org/10.1038/s43017-019-0001-x>
- Pocock, M. J. O., Evans, D. M., & Memmott, J. (2010). The impact of farm management on species-specific leaf area index (LAI): Farm-scale data and predictive models. *Agriculture, Ecosystems & Environment*, 135(4), 279-287. <http://doi.org/10.1016/j.agee.2009.10.006>
- 485 Potapov, P., Turubanova, S., Hansen, M. C., Tyukavina, A., Zalles, V., & Khan, A., et al. (2022). Global maps of cropland extent and change show accelerated cropland expansion in the twenty-first century. *Nature Food*, 3(1), 19-28. <http://doi.org/10.1038/s43016-021-00429-z>
- Propastin, P. A. (2009). Spatial non-stationarity and scale-dependency of prediction accuracy in the remote estimation of LAI over a tropical rainforest in Sulawesi, Indonesia. *Remote Sensing of Environment*, 113(10), 2234-2242. <http://doi.org/10.1016/j.rse.2009.06.007>
- 490 Querino, C. A. S., Beneditti, C. A., Machado, N. G., Da Silva, M. J. G., Da Silva Querino, J. K. A., & Dos Santos Neto, L. A., et al. (2016). Spatiotemporal NDVI, LAI, albedo, and surface temperature dynamics in the southwest of the Brazilian Amazon forest. *Journal of Applied Remote Sensing*, 10(2), 26007. <http://doi.org/10.1117/1.JRS.10.026007>
- Rusli, N., & Majid, M. R. (2014). Monitoring and mapping leaf area index of rubber and oil palm in small watershed area. *IOP conference series. Earth and environmental science*, 18(1), 12035-12036. <http://doi.org/10.1088/1755-1315/18/1/012036>
- 495 Satriawan, T. W., Luo, X., Tian, J., Ichii, K., Juneng, L., & Kondo, M. (2024). Strong Green-Up of Tropical Asia During the 2015/16 El Niño. *Geophysical Research Letters*, 51(8), e2023G-e106955G. <http://doi.org/https://doi.org/10.1029/2023GL106955>
- 500 Sitch, S., Friedlingstein, P., Gruber, N., Jones, S. D., Murray-Tortarolo, G., & Ahlström, A., et al. (2015). Recent trends and drivers of regional sources and sinks of carbon dioxide. *Biogeosciences*, 12(3), 653-679. <http://doi.org/10.5194/bg-12-653-2015>
- Sulla-Menashe, D., & Friedl, M. A. (2018). User guide to collection 6 MODIS land cover (MCD12Q1 and MCD12C1) product. *Usgs: Reston, Va, Usa*, 1, 18
- 505 Sulla-Menashe, D., Gray, J. M., Abercrombie, S. P., & Friedl, M. A. (2019). Hierarchical mapping of annual global land cover 2001 to present: The MODIS Collection 6 Land Cover product. *Remote Sensing of Environment*, 222, 183-194. <http://doi.org/10.1016/j.rse.2018.12.013>
- Takeshima, H. J. P. K. (2019). *Overview of the agricultural modernization in Southeast Asia*, Intl Food Policy Res Inst.
- Vernimmen, R. R. E., Bruijnzeel, L. A., Romdoni, A., & Proctor, J. (2007). Rainfall interception in three contrasting lowland rain forest types in Central Kalimantan, Indonesia. *Journal of Hydrology*, 340(3-4), 217-232. <http://doi.org/10.1016/j.jhydrol.2007.04.009>
- 510 Vijay, V., Pimm, S. L., Jenkins, C. N., Smith, S. J., & Anand, M. (2016). The Impacts of Oil Palm on Recent Deforestation and Biodiversity Loss. *PLoS One*, 11(7), e159668. <http://doi.org/10.1371/journal.pone.0159668>
- Wagner, M., Wentz, E. A., & Stuhlmacher, M. (2022). Quantifying oil palm expansion in Southeast Asia from 2000 to 2015: A data fusion approach. *Journal of land use science*, 17(1), 26-46. <http://doi.org/10.1080/1747423X.2021.2020918>
- 515 Wang, J. A., & Friedl, M. A. (2019). The role of land cover change in Arctic-Boreal greening and browning trends. *Environmental Research Letters*, 14(12), 125007. <http://doi.org/10.1088/1748-9326/ab5429>
- Wang, L., Zhao, Z., Zhang, K., & Tian, C. (2013). Reclamation and Utilization of Saline Soils in Arid Northwestern China: A Promising Halophyte Drip-Irrigation System. *Environmental Science & Technology*, 47(11), 5518-5519. <http://doi.org/10.1021/es4017415>
- 520

- Wang, X., Blanken, P. D., Kasemsap, P., Petchprayoon, P., Thaler, P., & Nouvellon, Y., et al. (2022). Carbon and Water Cycling in Two Rubber Plantations and a Natural Forest in Mainland Southeast Asia. *Journal of Geophysical Research: Biogeosciences*, 127(5). <http://doi.org/10.1029/2022JG006840>
- 525 Wang, Y., Hollingsworth, P. M., Zhai, D., West, C. D., Green, J., & Chen, H., et al. (High-resolution maps show that rubber causes substantial deforestation. *Nature*, 623(7986), 340-346. <http://doi.org/10.1038/s41586-023-06642-z>
- Watson, D. J. (1947). Comparative Physiological Studies on the Growth of Field Crops. I. Variation in Net Assimilation Rate and Leaf Area between Species and Varieties and between Years. *Annals of Botany*, 11, 41-76
- Wicke, B., Sikkema, R., Dornburg, V., & Faaij, A. (2011). Exploring land use changes and the role of palm oil production in Indonesia and Malaysia. *Land Use Policy*, 28(1), 193-206. <http://doi.org/10.1016/j.landusepol.2010.06.001>
- 530 Xu, Y., Yu, L., Li, W., Ciais, P., Cheng, Y., & Gong, P. (2020). Annual oil palm plantation maps in Malaysia and Indonesia from 2001 to 2016. *Earth System Science Data*, 12(2), 847-867. <http://doi.org/10.5194/essd-12-847-2020>
- Xu, Y., Ciais, P., Yu, L., Li, W., Chen, X., & Zhang, H., et al. (2021). Oil palm modelling in the global land surface model ORCHIDEE-MICT. *Geoscientific Model Development*, 14(7), 4573-4592. <http://doi.org/10.5194/gmd-14-4573-2021>
- 535 Xu, Y., Yu, L., Ciais, P., Li, W., Santoro, M., & Yang, H., et al. (2022). Recent expansion of oil palm plantations into carbon-rich forests. *Nature Sustainability*, 5(7), 574-577. <http://doi.org/10.1038/s41893-022-00872-1>
- Yan, F., Song, K., Liu, Y., Chen, S., & Chen, J. (2020). Predictions and mechanism analyses of the fatigue strength of steel based on machine learning. *Journal of Materials Science*, 55(31), 15334-15349. <http://doi.org/10.1007/s10853-020-05091-7>
- 540 Yang, C., Chen, M., & Yuan, Q. (2021). The application of XGBoost and SHAP to examining the factors in freight truck-related crashes: An exploratory analysis. *Accident Analysis & Prevention*, 158, 106153. <http://doi.org/10.1016/j.aap.2021.106153>
- Yang, Y., Xiao, X., Li, M., Dong, Z., & Zhao, R. (2024). A new framework for assessing carbon fluxes in alpine rivers. *Catena*, 246, 108423. <http://doi.org/10.1016/j.catena.2024.108423>
- 545 Yuan, W., Zheng, Y., Piao, S., Ciais, P., Lombardozi, D., & Wang, Y., et al. (2019). Increased atmospheric vapor pressure deficit reduces global vegetation growth. *Science Advances*, 5(8), x1396. <http://doi.org/10.1126/sciadv.aax1396>
- Zeng, Z., Estes, L., Ziegler, A. D., Chen, A., Searchinger, T., & Hua, F., et al. (2018). Highland cropland expansion and forest loss in Southeast Asia in the twenty-first century. *Nature Geoscience*, 11(8), 556-562. <http://doi.org/10.1038/s41561-018-0166-9>
- 550 Zhang, A., Liu, Y., Wang, F., Kong, D., Bi, J., & Zhang, F., et al. (2022). Molecular Breeding of Water-Saving and Drought-Resistant Rice for Blast and Bacterial Blight Resistance. *Plants (Basel)*, 11(19). <http://doi.org/10.3390/plants11192641>
- Zhao, H., Chang, J., Havlík, P., van Dijk, M., Valin, H., & Janssens, C., et al. (2021). China's future food demand and its implications for trade and environment. *Nature Sustainability*, 4(12), 1042-1051. <http://doi.org/10.1038/s41893-021-00784-6>
- 555 Zhao, J., Elmore, A. J., Lee, J. S. H., Numata, I., Zhang, X., & Cochrane, M. A. (2023a). Replanting and yield increase strategies for alleviating the potential decline in palm oil production in Indonesia. *Agricultural Systems*, 210, 103714. <http://doi.org/10.1016/j.agsy.2023.103714>
- 560 Zhao, R., Zhang, W., Duan, Z., Chen, S., & Shi, Z. (2023b). An improved estimate of soil carbon pool and carbon fluxes in the Qinghai-Tibetan grasslands using data assimilation with an ecosystem biogeochemical model. *Geoderma*, 430, 116283. <http://doi.org/10.1016/j.geoderma.2022.116283>
- Zhong, L., Ma, Y., Xue, Y., & Piao, S. (2019). Climate Change Trends and Impacts on Vegetation Greening Over the Tibetan Plateau. *Journal of Geophysical Research: Atmospheres*, 124(14), 7540-7552. <http://doi.org/10.1029/2019JD030481>
- 565 Zhu, Z., Piao, S., Myneni, R. B., Huang, M., Zeng, Z., & Canadell, J. G., et al. (2016). Greening of the Earth and its drivers. *Nature Climate Change*, 6(8), 791-795. <http://doi.org/10.1038/nclimate3004>